



$$P(p | \rho, T) = \frac{(\rho T)^p e^{-\rho T}}{p!} \quad (1)$$

where  $\rho$  is a rate parameter measured in photons per second. The mean and standard deviation are given by

$$\mu = \rho T \quad (2)$$

$$\sigma = \sqrt{\rho T} \quad (3)$$

Since the number of photons determines the intensity of a pixel, photon noise is not independent of the signal. In addition, photon noise is neither Gaussian nor additive. As shown in (2),  $\mu$  means the number of photons over interval  $T$ . It is natural that the number of photons in a brighter pixel is larger than that in a darker pixel.

We use a Poisson distribution directly to represent the distribution of intensity difference. The difference of two Poisson random variables is defined a Skellam distribution [8]. The probability mass function (pmf) of a Skellam distribution is a function of  $k$  which means difference between two Poisson random variables, and expressed as

$$P(k; \mu_1, \mu_2) = e^{-(\mu_1 + \mu_2)} \left( \frac{\mu_1}{\mu_2} \right)^{k/2} I_k(2\sqrt{\mu_1 \mu_2}) \quad (4)$$

where  $\mu_1$  and  $\mu_2$  are means or expected values of two Poisson distributions and  $I_k(z)$  is the modified Bessel function of the first kind.

We can estimate the Skellam parameters of intensity difference easily by using statistics of Skellam distribution. The mean  $\mu_S$  and the variance  $\sigma_S^2$  of a Skellam distribution are given as

$$\mu_S = \mu_1 - \mu_2 \quad (5)$$

$$\sigma_S^2 = \mu_1 + \mu_2 \quad (6)$$

From (5) and (6), we can calculate the parameters directly as

$$\mu_1 = (\mu_S + \sigma_S^2) / 2 \quad (7)$$

$$\mu_2 = (-\mu_S + \sigma_S^2) / 2 \quad (8)$$

$\mu_S$  and  $\sigma_S^2$  are obtained from images of a static scene like

$$\mu_S = \frac{\sum_t (x_t(i, j) - x_{t+1}(i, j))}{n} \quad (9)$$

$$\sigma_S^2 = \frac{\sum_t (\mu_S - (x_t(i, j) - x_{t+1}(i, j)))^2}{n} \quad (10)$$

where  $x_t(i, j)$  means the intensity of  $(i, j)$  position at frame  $t$  and  $n$  is the number of total images.

As noted previously, the parameters,  $\mu_1$  and  $\mu_2$  are the number of photons so that there might be a certain relationship between Skellam parameters and intensity. In [1], we showed that Skellam parameters and intensity have linearity. We called this line as the Intensity-Skellam line. If we estimate Intensity-Skellam line, we can estimate Skellam parameters for each pixel according to intensity of R, G, B channels.



Figure 1 Test image for Skellam-Intensity line estimation

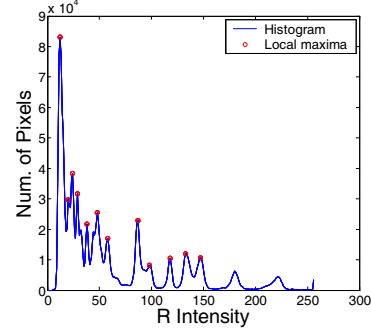


Figure 2 Intensity histogram and local maxima

### 3. Intensity-Skellam line estimation in the temporal domain

When we obtain some pairs of a Skellam parameter and intensity, we can fit a line to set of pairs. If we estimate Skellam parameters at a certain pixel in the temporal domain, we need more 10,000 images to ensure that the calculated statistics is sufficiently stable. But it is impractical to capture so many static images of indoor or outdoor images. We propose a new Intensity-Skellam line estimation method to reduce the required static images to two images. It is more practical compared with capturing over 10,000 images. When we assume that each pixel in an image is mutually independent, we can regard the intensity difference between two corresponding pixels in two frames as set of intensity difference in the temporal domain. Therefore, we have sufficient pixels at certain intensity for estimating Skellam parameters.

Our calibration algorithm for a channel is as follow.

1. Generate a histogram of intensity in first frame and find local maxima  $x_m^1$ ,  $m = 0, 1, \dots, M$
2. Find set of corresponding pixels in two frames around the local maxima as
 
$$X_m = \{x^1(i, j), x^2(i, j) | x_m - \varepsilon < x^1(i, j) < x_m + \varepsilon\}.$$
3. Calculate the mean and the variance of a Skellam distribution for each set  $X_m$ , as

$$\mu_S | X_m = \frac{\sum_{X_m} (x_k^1(i, j) - x_k^2(i, j))}{n},$$

$$\sigma_S^2 | X_m = \frac{\sum_{X_m} (\mu_S | X_m - (x_k^1(i, j) - x_k^2(i, j)))^2}{n}.$$

4. Calculate Skellam parameters,  $\mu_1$  and  $\mu_2$  from (7) and (8).
5. Fit two lines to pairs of  $(x_m^1, \mu_1)$  and  $(x_m^2, \mu_2)$  using conventional RANSAC methods.

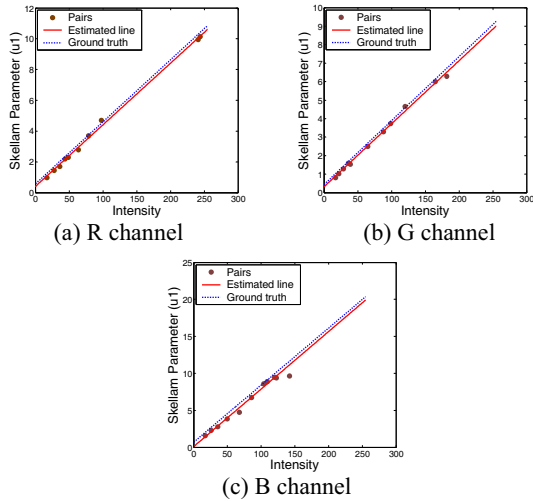


Figure 3 Intensity-Skellam line estimation results

We carry out an experiment on the algorithm for two real images as shown in Figure 1. We capture color patterns because we can obtain accurate Intensity-Skellam line from a large number of static images as ground truth. Figure 2 shows the histogram of intensity in the R channel and detected local maxima. From the local maxima, we have the pairs of intensity and Skellam parameters. We set the value of  $\mathcal{E}$  to one. The Intensity-Skellam line is determined by RANSAC. Figure 3 shows an estimation result for each channel. For comparison, we plot ground truth lines obtained by 10,000 static images. Our Intensity-Skellam line is very accurate compared with the ground truth. Most of the pairs used for fitting lines are laid around the fitted line. It means that we can estimate the line by using small number of pairs.

## 4. Background subtraction

### 4.1. Maintenance of the background image

When we measure the difference between only consecutive frames, we can not deal with various situations that can be occurred in general indoor and outdoor environment such as abrupt or gradual illumination changes, position changes of furniture and moving vehicles are stopped or parked. Therefore, we should maintain a background image to deal with such environmental changes.

There are two conventional mechanisms to update background. First one is a selective update which adds the new pixel to the model only if it is classified as a background pixel. From this approach, we can correct the part of backgrounds occluded by moving objects at previous frames. But the problem is that erroneous detection results or temporary static objects may make permanent incorrect background model. It causes the incorrect foreground detection at incorrect background parts. Second one is a blind update which just adds the new sample to the model. This update can reduce the previous problem of the selective update since it restores the incorrect background model to correct one. But it causes another problem of updating incorrect background model by moving objects and false alarms.

In order to deal with these problems of conventional update methods, we propose another background model-

ing strategy. The conventional update methods [5] used only background images and current upcoming images. But we utilize difference between two consecutive images to update the background model. Our algorithm of maintaining the background model is as follows:

1. Initialize a background image,  $I_B^0(p)$ , as an image in the first frame.
2. For each frame  $t$ , store history images of length  $T$  and update background mask as

$$M^t(p_B) = 1, M^t(p_F) = 0.$$

( $P_B, P_F$ : Classified as a background and a foreground pixel in consecutive images, respectively)

3. If  $t \geq T$ , update the background model as

$$I_B^t(p) = \begin{cases} \sum_{i=t-T}^t I_H^i(p), & \text{if } \prod_{i=t-T}^t M_i(p) = 1 \\ I_B^{t-1}(p), & \text{otherwise} \end{cases}$$

( $I_H^i$  is a stored history image at frame  $i$ ).

Our algorithm can deal with the problems of selective and blind updates. We can correct the part of backgrounds occluded by moving objects the same as the selective update. The problem of a blind update is solved because we update the incorrect background parts when there is no foreground during  $T$  frames. Therefore, we don't need the blind update to restore the incorrect parts. The only defect is that it takes  $T$  frames to update the background correctly. When we set  $T=1$ , our algorithm became totally same as a selective update. Otherwise, our algorithm corrects the erroneous parts within  $T$  frames.

### 4.2. Background subtraction strategy

From Section 3, we have exact distributions for each pixel in the image. We can classify foregrounds to measure the difference between a current image and the maintained background image from Section 4.1. The update parameter  $T$  is set to five. The classification is performed by a statistical hypothesis test [9]. Our noise modeling is so precise that subtraction results have few false alarms as shown in Figure 4. Therefore, we do not need to any further processing as shown in other methods [5]. Our background update algorithm is applicable since the result is almost the true foregrounds.

## 5. Experimental results

We apply our algorithm to an outdoor sequence. We use PointGrey Flea camera with a 640x480 resolution. Our algorithm runs by 4Hz in AMD Athlon64 X2 2.41GHz and 2GB memory. In Figure 4(b), we show updated background images given current images as shown in Figure 4(a). Although there are moving objects, our background model can adapt the background well. Based on updated backgrounds we can detect foreground parts by measuring the difference between current upcoming images and background images. In Figure 4(c), detection results are so accurate that our method can de-

tect almost true boundaries for moving humans and cars except for a few shadows. Compared with the result by mixture of Gaussian [4], our results have smaller missing pixels as well as smaller false alarms because mixture of Gaussian can not guarantee exact distribution of pixel color differences but have rough Gaussian distributions for background estimation. The third column result shows a scene change by an abrupt illumination change. Since our background model is promptly adapted, false alarms are much reduced than the result from mixture of Gaussian. Furthermore, our all of pixels have exact distribution according to intensity, we can detect moving objects in the dark condition as shown in Figure 5.

It is worthy noted that all of our detection results have pretty small false alarms as shown in Figures 4 and 5. It is very advantageous to apply surveillance system. Most of subtraction algorithm suffered from false alarms as shown in third column of Figure 4(d). It is difficult to discriminate the real foreground caused by moving human or cars from the false alarms caused by misclassification. But, our results have small false alarms although we do not use any further post processing. Therefore, we can determine that there is some foreground pixels in our detection result, most of them are caused by real moving objects.

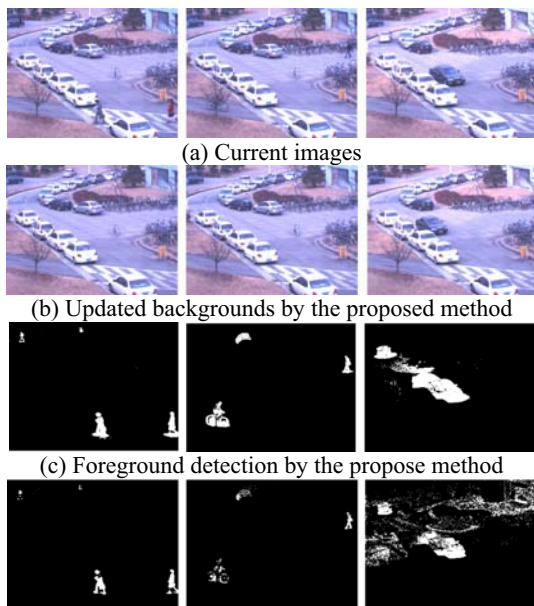


Figure 4 Background subtraction results (daylight)

## 6. Conclusions

We propose a new background subtraction method by using previously proposed noise modeling and a new background update strategy. Other previous methods deal with background subtraction with approximated distributions because they can not define an exact difference for classification. But we can define an exact difference based on sensor noise modeling. To estimate Intensity-Skellam line, we propose an estimation method for two static images. The line estimation result is so accurate that there is little difference with the available ground truth. We propose a background update approach. Conventional methods used only the difference between an input image and a background image to update the

background model. In the contrary, we utilize the difference between consecutive frames for updating backgrounds. Our background update method adapts the change of backgrounds very well. Based on estimated noise statistics and updated background models, we can detect foreground parts precisely in sequences. The advantage of our method is that there are few false alarms without post processing and we can apply our algorithm for dark conditions.

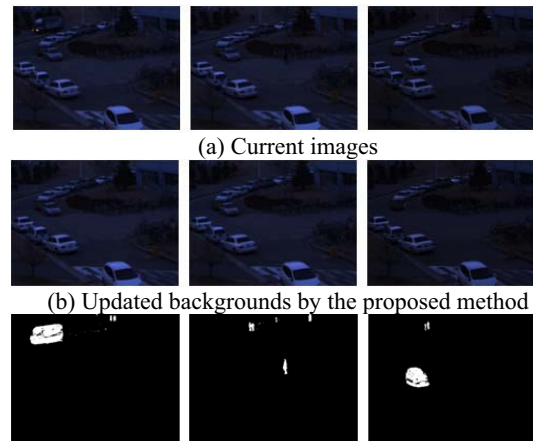


Figure 5 Background subtraction results (dark)

## Acknowledgement

This research has been supported by the Korean Ministry of Science and Technology for National Research Laboratory Program (Grant number M1-0302-00-0064).

## References

- [1] Youngbae Hwang, Jun-Sik Kim and In-So Kweon, "Sensor noise modeling using the Skellam distribution: Application to the color edge detection", In Int. Conf. on CVPR, 2007, to appear
- [2] C. Wren, A. Azarbayejani, T. Darrel, and A. Pentland, "Pfinder: Real-time tracking of the human body", IEEE Trans. on PAMI, vol.19, no.7, pp.780-785, 1997
- [3] N. Friedman and S. Russel, "Image segmentation in video sequences: A probabilistic approach", In Conf. on Uncertainty in Artificial Intelligence (UAI), pp.175-181, 1997
- [4] C. Stauffer and W. Grimson, "Learning patterns of activity using real-time tracking", IEEE Trans. on PAMI, vol. 22, pp.747-757, 2000
- [5] A. Elgammal, D. Harwood and L. Davis, "Non-parametric model for background subtraction", pp.751-767, In European Conf. on Computer Vision, 2000
- [6] A. Mittal and N. Paragios, "Motion-based background subtraction using adaptive kernel density estimation", In Int. Conf. on CVPR, pp.302-309, 2004
- [7] I. Young, J. Gerbrands, and L. van Vliet, "Fundamentals of image processing", 1995, Delft University of Technology
- [8] J. G. Skellam, "The frequency distribution of the difference between two Poisson variates belonging to different populations", Journal of the Royal Statistical Society: Series A, vol.109, no.3, pp.296, 1946
- [9] E. R. Dougherty. Probability and statistics for the engineering, computing and physical sciences. Prentice Hall, 1990